molbank

MDPI

Short Note

2-(1*H*-Imidazol-2-yl)-2,3-dihydro-1*H*-perimidine

Zhanina Petkova [1], Rusi Rusew [2], Snezhana Bakalova [1], Boris Shivachev [2,*] and Vanya Kurteva [1,*]

[1] Institute of Organic Chemistry with Centre of Phytochemistry, Bulgarian Academy of Sciences, Acad. G. Bonchev Street, bl. 9, 1113 Sofia, Bulgaria
[2] Institute of Mineralogy and Crystallography "Acad. Ivan Kostov", Bulgarian Academy of Sciences, Acad. G. Bonchev Street, bl. 107, 1113 Sofia, Bulgaria
* Correspondence: blshivachev@gmail.com (B.S.); vanya.kurteva@orgchm.bas.bg (V.K.)

Abstract: The novel compound 2-(1H-imidazol-2-yl)-2,3-dihydro-1H-perimidine was obtained in very good yield via a known eco-friendly protocol. The product was isolated in pure form as a solvate by simple filtration from the crude mixture. Its structure was assigned by 1D and 2D NMR experiments and was confirmed by high resolution MS and single crystal XRD. The temperature of methanol release was determined by DSC and the energy of the process theoretically estimated.

Keywords: 2,3-dihydro-1H-perimidine; 2-imidazolyl; methanol solvate; NMR; single crystal XRD

Citation: Petkova, Z.; Rusew, R.; Bakalova, S.; Shivachev, B.; Kurteva, V. 2-(1*H*-Imidazol-2-yl)-2,3-dihydro-1*H*-perimidine. *Molbank* **2023**, *2023*, M1587. https://doi.org/10.3390/M1587

Academic Editor: Kristof Van Hecke

Received: 31 January 2023
Revised: 10 February 2023
Accepted: 13 February 2023
Published: 15 February 2023

1. Introduction

Perimidines are π-amphoteric tricyclic aromatic heterocycles [1] with a broad variety of applications [2–6]. The most synthetic protocols present a one-pot two-step procedure; formation of dihydroperimidines followed by dehydration [7,8]. The intermediate dihydroperimidines also exhibit a diverse range of properties; some examples are shown in Figure 1.

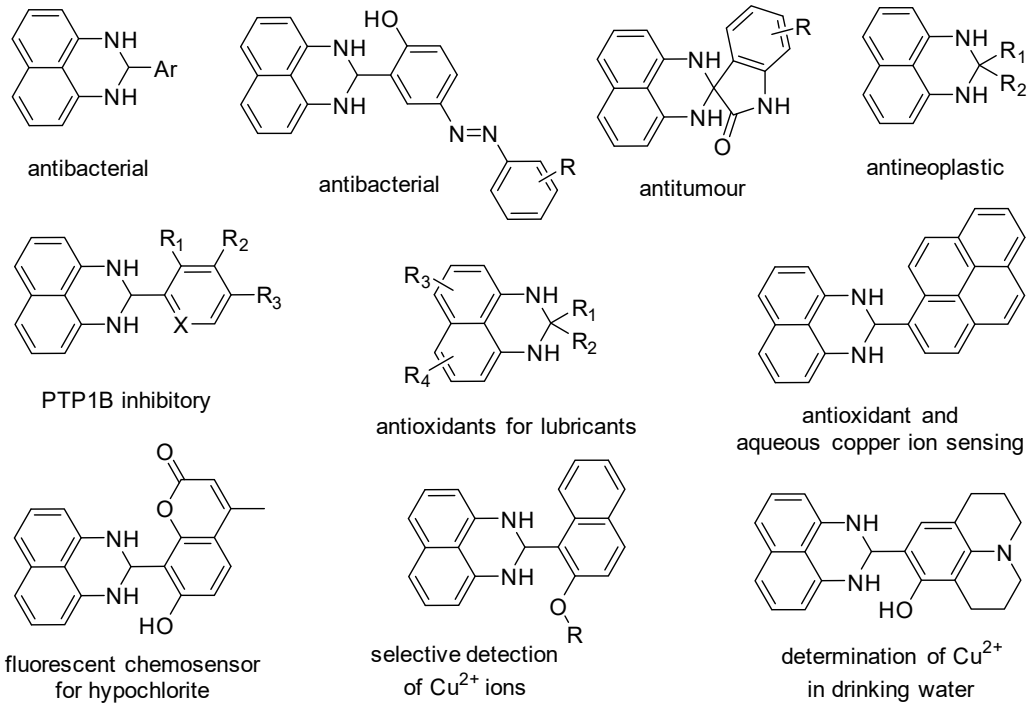

Figure 1. Representatives of 2,3-dihydro-1H-perimidine derivatives showing various applications.

Numerous derivatives display variable bioactivities, such as antibacterial [9,10], anti-tumor [11], anti-neoplastic [12], PTP1B inhibitory [13], etc., and applications such as

chemosensors for hypochlorite [14] and Cu^{2+} ions [15–17], carbene pincer ligands [18–21], antioxidants for lubricants [22], and many others. Among the protocols for the synthesis of 2,3-dihydroperimidines, the condensation between naphthalene-1,8-diamines and carbonyl compounds, mainly aldehydes, is relatively simple and so economically relevant that it practically has no alternative and has been intensively exploited. For that reason, the main attempts of scientific groups have been directed towards the synthesis of a broad variety of derivatives by development of efficient catalysts [23–31].

Recently, we reported on the synthesis and anticancer activity of a series of perimidines [32], including the new 2-imidazolyl derivative. As a continuation, we focused our attention on their precursors, the corresponding dihydro-analogues. Therefore, we present herein the synthesis and solution and solid-state characterization of a novel dihydroperimidine compound, 2-(1H-imidazol-2-yl)-2,3-dihydro-1H-perimidine.

2. Results and Discussion

2.1. Synthesis

The novel dihydroperimidine derivative 2-(1H-imidazol-2-yl)-2,3-dihydro-1H-perimidine is obtained via a simple eco-friendly protocol, shown in Scheme 1. The condensation between 1,8-diaminonaphthalene and imidazole-2-carbaldehyde is carried out at room temperature in various solvents, such as acetonitrile, THF, methanol, and even water according to a recently reported procedure [33]. The best results, 88% yield and easy work-up, are obtained in methanol for two main reasons. On the one hand, both reagents have good solubility in alcohols, while the limited solubility of bis-amine in acetonitrile and THF resulted in relatively low yields after significant reaction prolongation, and no conversion was detected in water where both compounds are completely insoluble. On the other hand, the target product possesses limited solubility in methanol at room temperature allowing its isolation in pure form by simple filtration of the crude reaction mixture.

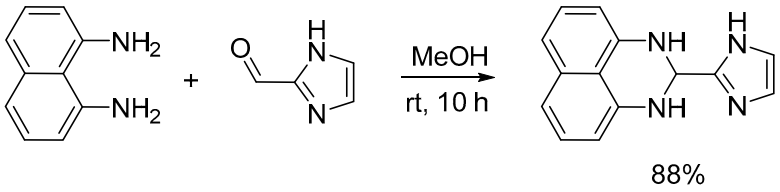

Scheme 1. Synthesis of 2-(1H-imidazol-2-yl)-2,3-dihydro-1H-perimidine.

The structure of the product was assigned by 1D and 2D NMR spectra (see Supporting Information). The ^{1}H spectrum in DMSO-d_6 shows characteristic signals for the aromatic perimidine protons; two doublets of doublets with ^{3}J and ^{4}J at 6.529 and 7.009 ppm for C*H*-4+9 and C*H*-6+7, respectively, and a doublet with two ^{3}J for C*H*-5+8 at 7.160 ppm. The C*H*-2 connecting both fragments appears as a singlet at 5.470 ppm, while both N*H* protons give a singlet at 6.832 ppm. The imidazolyl unit shows two very broad singlets at 6.910 and 7.133 ppm for C*H* protons, most probably due to slow exchange, and a broad singlet at 12.277 ppm for N*H*. The assignment of the signals was based on the characteristic interactions in a NOESY experiment, namely N*H*/C*H*-4+9, N*H*/C*H*-2 and imidazolyl N*H* with both broad singlets for C*H*. ^{13}C spectrum shows a signal for *C*H-2 at 62.03 ppm, three intensive signals for perimidine *C*H-4+9, *C*H-6+7, and *C*H-5+8 at 105.21, 116.09, and 127.29 ppm, respectively, two signals with very low intensities for imidazolyl *C*H at 117.68 and 127.45 ppm and four signals for quaternary carbons. The latter are assigned as C_q-3a^{1} at 113.03 ppm, C_q-6a at 134.75 ppm, C_q-3a+9a at 142.99 ppm, and C_q-2 of imidazolyl unit at 147.43 ppm by analysing the specific interactions in an HMBC experiment. The product's structure was confirmed by high resolution mass-spectra, where molecular ions were detected in both positive and negative mode.

The NMR spectra also show signals for a hydrogen bonded molecule of methanol (1:1 ratio product/MeOH); doublet at 3.173 ppm for CH_3 and quartet at 4.114 ppm for O*H* in the proton spectrum and a signal for methyl carbon at 49.06 ppm. This pattern is valid

for both crude and recrystallised from methanol products. The methanol O*H* quartet and CH_3 doublet gave negative correlations in a NOESY experiment with both imidazolyl C*H* protons and with O*H*, respectively, all possessing very low intensities as expected due to the broad imidazolyl signals detected in the proton spectrum. Based on these observations, it can be concluded that the product forms stable 1:1 solvate both during its preparation and recrystallization.

The DSC data (Figure 2a) disclose that the methanol molecules start to leave the crystal structure around 60 °C and the process is complete around 110 °C (the calculated H is 193 kJ/mol). According to the DSC data the solvent release is not accompanied by a phase transition and the next endothermic effect is the melting of the compound (H = 84 kJ/mol). The thermogravimetric data visualizing the mass losses observed during heating of the title compound are shown on Figure 2b. The registered weight loss up to 110 °C is ~13 wt% and correlates with the theoretical estimations for methanol release (12%). After 180 °C the TG registers the losses associated to the melting and evaporation of the title compound.

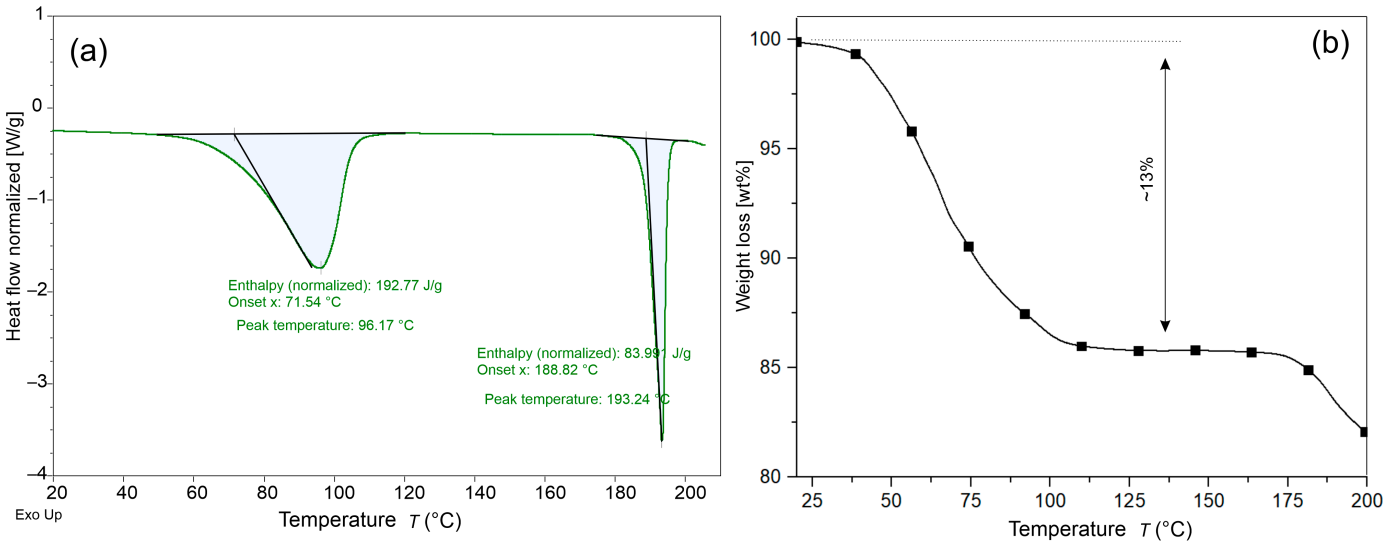

Figure 2. Thermal analysis of the title compound. (**a**) DSC thermogram of the title compound disclosing two endothermic effects associated with the release of methanol (60–110 °C) and (**b**) TGA data reveling a weight loss of ~13% corresponding to methanol molecule.

2.2. Crystallography

The title compound 2-(1H-imidazol-2-yl)-2,3-dihydro-1H-perimidine appears as pale beige-coloured prisms obtained by slow-evaporation from methanol. The crystal structure of the studied compound was solved in the monoclinic $P2_1/c$ space group with cell parameters – a = 11.5777(9) Å, b = 9.2885(11) Å, c = 13.9591 Å and β = 113.472(3)° (Table S1). The compound crystallizes as a crystal solvate as one molecule methanol is entrapped in the crystal structure (four molecules per unit cell). A close inspection of the molecular features reveals that 2-(1H-imidazol-2-yl)-2,3-dihydro-1H-perimidine is built up of two main fragments: 2,3-dihydro-1H-perimidine (fragment 1) and 1H-imidazole (fragment 2) connected by a single –(H)C–C– covalent bond (namely C6–C5, see Figure 3). Furthermore, fragment 1 consists of a planar (r.m.s.d = 0.037Å) naphthalene ring system and a six membered hetero ring formed by the mutual C8–C18–C16 atoms of the naphthalene backbone and a N–C(H)–N group. The hetero ring is in an envelope conformation with the N–C–N group hinged with respect to the naphthalene ring at 49.86(16)°. The imidazole moiety is actually planar (r.m.s.d = 0.001 Å) and the mean plane between the two ring systems (1H-perimidine and imidazole) is 95.74(7)°.

The crystal structure of 2-(1H-imidazol-2-yl)-2,3-dihydro-1H-perimidine is stabilized by three types of hydrogen bonding interactions: O–H…N, N–H…O, and N–H…N. The first type is represented by the strongest hydrogen bonding interaction (D…A distance of 2.731 Å) between the N4 atom of fragment 2 and the methanol molecule. The second type

(N-H…O) is represented by two distinct hydrogen bonding interactions involving the two N–H groups 1H-perimidine N17–H17…O19 and N7–H7…O19 – with D…A distances of 3.005 and 3.047 Å, respectively. The third type of hydrogen bonding interactions (N–H…N) involves the N1-H1…N7 atoms of imidazole and 1H-perimidine from adjacent molecules. This leads to the formation of dimmers through $R(_2^2)10$ motifs and chains propagating along *c* (Figure 4). The comparison of the recovered powder diffraction pattern (Figure S1) and that calculated from single crystal data show that the title compound is monophasic with high purity.

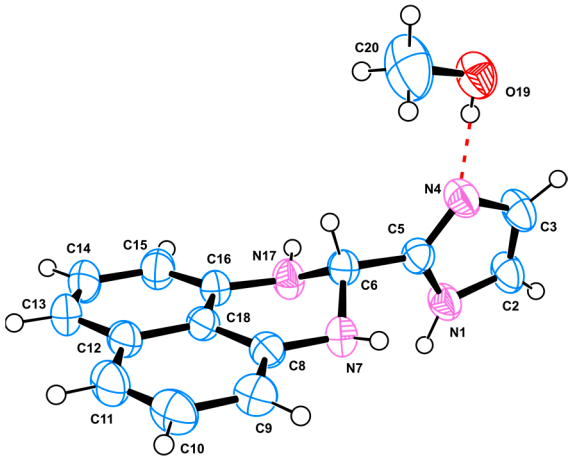

Figure 3. A representation of the molecules present in the asymmetric unit of the title compound along with the employed numbering scheme; atomic displacement parameters (ADP) are at 50% probability level, hydrogen atoms are shown as small spheres with arbitrary radii.

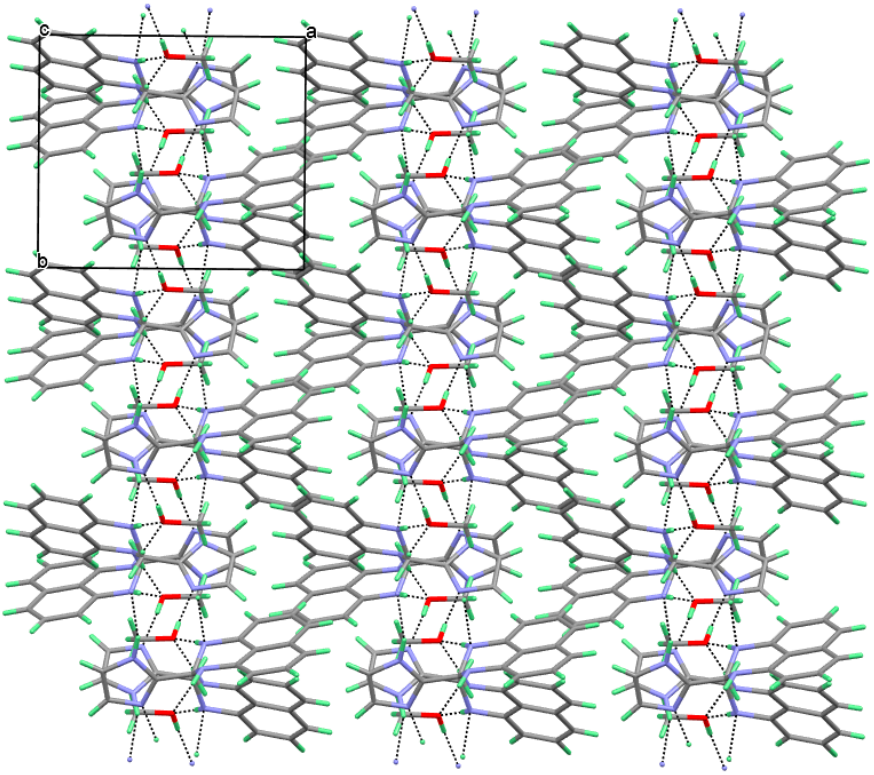

Figure 4. Observed hydrogen bonding interactions stabilizing the crystal packing in the title compound.

The networks of hydrogen bonds assemble the 2-(1H-imidazol-2-yl)-2,3-dihydro-1H-perimidine and methanol into a quite stable chain architecture (Figure 4, Table 1). Indeed,

the NMR data in solution also expose the presence of the MeOH…imidazole interaction. This fact suggested that the named interaction may be quite energetic, e.g., the formed hydrogen bond should be stronger than the three other ones detected. This hypothesis is supported by the comparison of D…A distances (2.733 to 3.047 Å) where the O19–H19…N4 is the shortest (2.733 Å). In an attempt to explain this observation, we generated intermolecular framework interactions for methanol…2-(1H-imidazol-2-yl)-2,3-dihydro-1H-perimidine and calculated their corresponding interaction energies (Table 2). The calculated energies (Table 2) were compared with the experimentally obtained enthalpy of methanol release (193 J/g, Figure 2). The computed "hydrogen bonding" interaction values are shown in Table 2. Again, the strongest one (–34.6 kJ/mol) is between MeOH and the imidazole moiety. The 1H-perimidine…MeOH interaction energies with values of –28.7 and –23.3 kJ//mol are slightly weaker but not significantly when compared to –34.6 kJ/mol. The last computed interaction energy (N1H1…N7, –83.2 kJ/mol) could be related to the melting effect of the compound.

Table 1. Observed hydrogen bonding interactions in the title compound.

D	H	A	d(D-H)/Å	d(H-A)/Å	d(D-A)/Å	D-H-A/°
O19	H19	N4	0.89(3)	1.84(3)	2.731(2)	175(3)
N1	H1	N71	0.94(3)	2.13(3)	3.035(3)	162(2)
N7	H7	O192	0.81(2)	2.19(2)	3.005(2)	177(2)
N17	H17	O193	0.87(3)	2.19(3)	3.047(3)	170(2)
11-x,2-y,1-z; 21-x,1/2+y,3/2-z;31-x,1-y,1-z						

Table 2. Interaction energies (kJ/mol) computed using single crystal geometries.

	R	Electron Density	E_{ele}	E_{pol}	E_{dis}	E_{rep}	E_{tot}
O19H19…N4	4.99	B3LYP/6-31G(d,p)	−62.3	−14.6	−11.6	84.5	−34.6
N17H17…O19	4.63	B3LYP/6-31G(d,p)	−21.4	−5.3	−15.1	26.5	−23.3
N7H7…O19	4.60	B3LYP/6-31G(d,p)	−28.0	−6.5	−16.5	32.5	−28.7
N1H1…N7	5.23	B3LYP/6-31G(d,p)	−70.1	−16.8	−60.6	90.7	−83.2

The experimentally observed endothermic release of methanol is accompanied by the destruction of the hydrogen bond interactions plus the energy for the evaporation of methanol (35 kJ/mol). A comparison between the DSC enthalpy (experimental 51.7 kJ/mol) and computed interactions energies (SUM of energies, 63.9 kJ/mol) suggests that the computed interaction energies appear to be overestimated by ~10% but reproduce correctly the strength of the various interactions.

Finally, a brief comparison between the product and its dehydrogenated analogue, 2-(1H-imidazol-2-yl)-1H-perimidine [32]. Both compounds are methanol insoluble, but the latter does not form a similar solvate (Figure 5) despite the last purification step being trituration with methanol. This difference could be explained by a delocalization of the imidazolyl N*H* in the aromatic molecule, while in dihydroperimidine it is located on the imidazolyl unit due to the absence of conjugation.

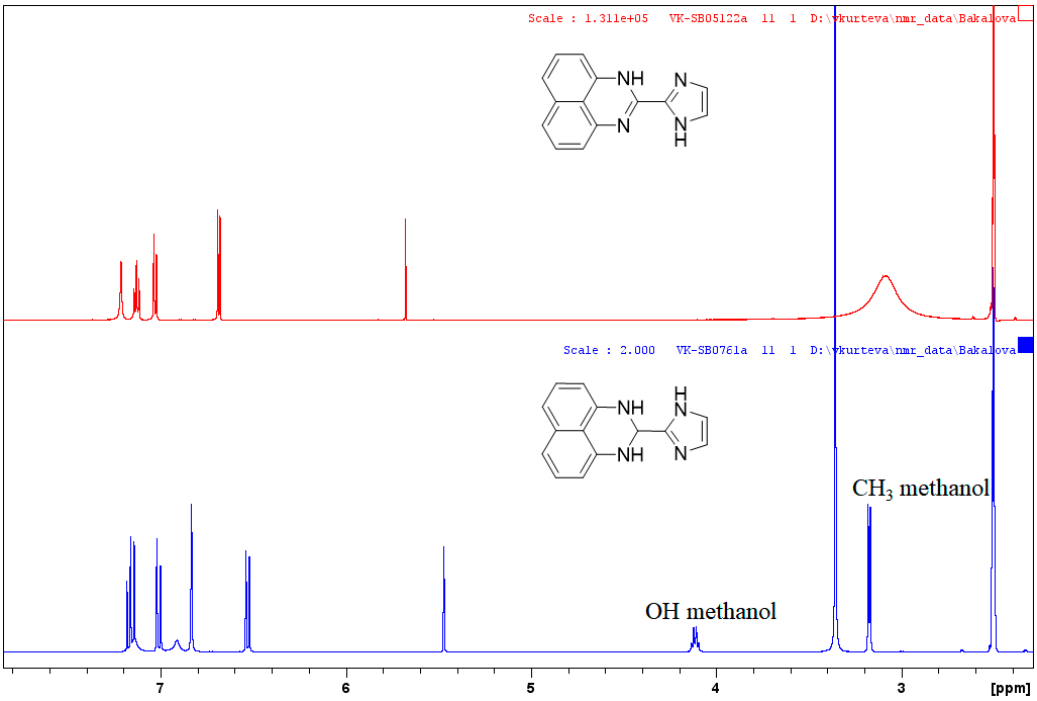

Figure 5. ^{1}H NMR spectra of 2-(1H-imidazol-2-yl)-2,3-dihydro-1H-perimidine (down) and 2-(1H-imidazol-2-yl)-1H-perimidine (up) in DMSO-d_6.

3. Materials and Methods

3.1. General

All reagents were purchased from Aldrich, Merck and Fluka and were used without any further purification. The deuterated dimethylsulfoxide was purchased from Deutero GmbH. Fluka silica gel (TLC-cards 60778 with fluorescent indicator 254 nm) plates were used for TLC chromatography and R_f-value determination. The melting point was determined in a capillary tube on SRS MPA100 OptiMelt (Sunnyvale, CA, USA) automated melting point system with heating rate of 1 °C per min. The NMR spectra were recorded on a Bruker Avance NEO 400 spectrometer (Rheinstetten, Germany) in DMSO-d_6; the chemical shifts are quoted in ppm in δ-values against the solvent peak at 2.5 ppm and the coupling constants were calculated in Hz. The assignment of the signals was confirmed by applying two-dimensional NOESY, HSQC, and HMBC techniques. The spectra were processed with the Topspin 3.6.3 program. For simplicity, the imidazole nuclei are depicted as "Im". The IR spectrum was measured on a Shimadzu IR Spirit FT-IR spectrometer (Shimadzu Corporation, Kyoto, Japan, USA) using QATR-S as a single-reflection ATR measurement attachment. The mass spectra were recorded in both positive and negative mode on a Q Exactive Plus Hybrid Quadrupole-Orbitrap Mass Spectrometer Thermo Scientific (ESI HR-MS). The spectra were processed with Xcalibur Free Style program version 4.5 (Thermo Fisher Scientific Inc., Waltham, MA, USA). DSC analyses were performed on a Discovery DSC250 (TA Instruments, New Castle DE, USA). Samples weighing between 1 and 5 mg were heated in aluminum pans from 20 to 350 °C (10 °C·min^{-1}) in nitrogen (flow rate 25 mL·min^{-1}). The enthalpy values (9 J/g) of the endothermic effects (methanol release) and melting of the synthesized compound were determined from indium melting calibration. Thermogravimetric analyzes were performed using a Q50 analyzer (TA Instruments). Ten mg of sample was placed in a ceramic container and measurements were made in the temperature range of 20 to 200 °C with a heating rate of 10 °C·min^{-1} under a nitrogen flow rate of 25 mL·min^{-1}.

3.2. Synthesis of 2-(1H-Imidazol-2-yl)-2,3-Dihydro-1H-Perimidine (1:1 MeOH Solvate)

A solution of 1,8-diaminonaphthalene (2 mmol) and imidazole-2-carbaldehyde (2 mmol) in MeOH (10 mL) was stirred at rt for 10 h. The solid phase formed was filtered off and washed with small portions of cold MeOH to give the pure product: 88% yield; R_f 0.17 (5% MeOH in DCM); pale beige solid; m. p. 186.1–186.3 °C; ^{1}H NMR 3.173 (d, 3H, J 5.0, C*H*$_3$ MeOH), 4.114 (q, 1H, J 5.0, O*H* MeOH), 5.470 (s, 1H, C*H*-2), 6.529 (dd, 2H, J 7.4, 0.6, C*H*-4+9), 6.832 (s, 2H, N*H*-1+3), 6.911 (s, 1H, CH Im), 7.009 (dd, 2H, J 8.2, 0.6, C*H*-6+7), 7.133 (s, 1H, CH Im), 7.160 (dd, 2H, J 8.0, 7.6, C*H*-5+8), 12.277 (s, 1H, N*H* Im); ^{13}C NMR 49.06 (*C*H$_3$ MeOH), 62.03 (*C*H-2), 105.21 (*C*H-4+9), 113.03 (*C*$_q$-3a^1), 116.09 (*C*H-6+7), 117.68 (*C*H Im), 127.29 (*C*H-5+8), 127.45 (*C*H Im), 134.75 (*C*$_q$-6a), 142.99 (*C*$_q$-3a+9a), 147.43 (*C*$_q$ Im); IR (ATR) 3206, 3111, 3052, 2804, 1600, 1518, 1459, 1406, 1376, 1265, 1164, 1121, 1108, 1087, 1070, 856, 819, 756, 723, 628, 441 cm^{-1}; HRMS (ESI$^+$) *m*/*z* calcd. for $C_{14}H_{13}N_4^+$ [M+H]$^+$ 237.1135, found 237.1133, Δ = −0.2 mDa; HRMS (ESI$^-$) *m*/*z* calcd. for $C_{14}H_{11}N_4^-$ [M-H]$^-$ 235.0978, found 235.0980, Δ = 0.2 mDa.

3.3. Crystallography

Pale beige coloured crystal blocks from the titled compound were obtained by recrystallization from methanol. Suitable crystals with appropriate sizes (0.25 × 0.2 × 0.18 mm^3) were mounted on a nylon loop using cryoprotective Paratone oil. Diffraction data were collected on a Bruker D8 Venture diffractometer equipped with IμS micro-focus sealed X-ray source (MoKα radiation, λ = 0.71073 Å) and a PHOTON II CPAD detector. Diffraction data were processed in the APEX4 software package [34]; peaks were integrated with the Bruker SAINT software [35] using a narrow-frame algorithm. Intensities were scaled and the data corrected for absorption effects using the Multi-Scan method (SADABS) [35]. The structure was solved with the intrinsic phasing method and refined by the full-matrix least-squares method on F^2 (ShelxT and ShelxL program packages [36,37]) using OLEX—ver. 1.5 software [38]. All non-hydrogen atoms were located successfully from the Fourier map and were refined anisotropically. Hydrogen atoms were placed on calculated positions riding on the parent carbon atoms using the following scheme: U_{eq} = 1.2 for C–H$_{aromatic}$ = 0.93 Å, C–H$_{methyl}$ = 0.96 Å. ORTEP-3v2 software [39] was used to illustrate the molecules present in the asymmetric unit. Three-dimensional packing and visualization of the molecules of the title compound was made using CCDC Mercury [40]. The most important data collection and crystallographic refinement parameters for **3** are given in Table S1. Complete crystallographic data for the reported structure were deposited in the CIF format with the Cambridge Crystallographic Data Centre as 2215392. These data can be obtained free of charge via http://www.ccdc.cam.ac.uk/conts/retrieving.html, deposited on 26 October 2022, (or from the CCDC, 12 Union Road, Cambridge CB2 1EZ, UK; Fax: +441223336033; E-mail: depos-it@ccdc.cam.ac.uk).

The diffraction patterns of powdered samples and computed from SCXRD data were compared to establish the crystalline properties, purity, and eventual presence of additional phases. Powder XRD patterns were collected from the ground residue of the title compound (manually in an agate mortar). The ground (powder) sample of the synthesized compound was placed in a zero background holder and data were collected on an Empyrean Powder X-ray diffractometer (Malvern Panalytical, The Netherlands) in the 2–50° 2θ range using Cu radiation (λ = 1.5406 Å) and a PIXcel3D detector (Figure S1).

3.4. Computational Studies

Intermolecular frameworks for the title compound were generated from the crystal structure (CIF) with Crystalexplorer 21.5 [41] and the corresponding interaction energies calculated for all unique molecular pairs methanol…2-(1H-imidazol-2-yl)-2,3-dihydro-1H-perimidine using experimental crystal geometries; energies were calculated at CE-B3LYP…B3LYP/6-31G(d,p) level [42] using Tonto [43].

4. Conclusions

2-(1H-Imidazol-2-yl)-2,3-dihydro-1H-perimidine was obtained in high yield by condensation between 1,8-diaminonaphthalene and imidazole-2-carbaldehyde. The product was isolated by simple filtration and characterized by 1D and 2D NMR, IR, and HRMS spectra. The single crystal XRD indicates that the compound crystallizes in the monoclinic $P2_1/c$ space group. It was found that the product forms stable 1:1 solvate both in solution and solid state. DSC revealed that the methanol molecule leaves the crystal structure in the temperature interval 60–110 °C without phase transition and the energy of its release was theoretically estimated to be around 35 kJ/mol.

Supplementary Materials: The following supporting information can be downloaded online, Figure S1: Comparison of powder diffractogram (red) and calculated (blue) from single crystal data for 4ClB:Pro co-crystals; Figure S2: 1H NMR spectrum of 2-(1H-imidazol-2-yl)-2,3-dihydro-1H-perimidine in DMSO-d6; Figure S3: Partial 1H NMR spectrum of 2-(1H-imidazol-2-yl)-2,3-dihydro-1H-perimidine in DMSO-d6; Figure S4: NOESY spectrum of 2-(1H-imidazol-2-yl)-2,3-dihydro-1H-perimidine in DMSO-d_6; Figure S5: Partial NOESY spectrum of 2-(1H-imidazol-2-yl)-2,3-dihydro-1H-perimidine in DMSO-d_6; Figure S6: ^{13}C NMR spectrum of 2-(1H-imidazol-2-yl)-2,3-dihydro-1H-perimidine in DMSO-d_6; Figure S7: HSQC spectrum of 2-(1H-imidazol-2-yl)-2,3-dihydro-1H-perimidine in DMSO-d_6; Figure S8: HMBC spectrum of 2-(1H-imidazol-2-yl)-2,3-dihydro-1H-perimidine in DMSO-d_6; Figure S9: IR spectrum of 2-(1H-imidazol-2-yl)-2,3-dihydro-1H-perimidine; Figure S10: HRMS spectrum in positive mode (ESI^+); Table S1: The most important data collection and crystallographic refinement parameters.

Author Contributions: The conceptualization belongs to S.B. and V.K. The synthetic experiments and NMR analyses were carried out by V.K. The ESI HR-MS spectra were conducted by Z.P. The DSC, TGA single crystal and powder XRD were performed by R.R. and B.S. The calculations were determined by B.S. All authors contributed to the discussion of the results and in the manuscript writing. All authors have read and agreed to the published version of the manuscript.

Funding: This research is funded by the Bulgarian National Science Fund, project DN 19/11.

Data Availability Statement: Not applicable.

Acknowledgments: The financial support by the Bulgarian National Science Fund, project DN 19/11 from 10 December 2017, is gratefully acknowledged.

Conflicts of Interest: The authors declare no conflict of interest.

Sample Availability: Samples of the compounds are not available from the authors.

References

1. Pozharskii, A.F.; Gulevskaya, A.V.; Claramunt, R.M.; Alkorta, I.; Elguero, J. Perimidines: A unique π-amphoteric heteroaromatic system. *Russ. Chem. Rev.* **2020**, *89*, 1204–1260. [CrossRef]
2. Gümüş, M.; Gümüş, N.; Eroğlu, H.E.; Koca, İ. Design, synthesis and cytotoxic activities of pyrazole-perimidine hybrids. *Chem. Sel.* **2020**, *5*, 5916–5921. [CrossRef]
3. Farghaly, T.A.; Al-Hussain, S.A.; Muhammad, Z.A.; Abdallah, M.A.; Zaki, M.E.A. Synthesis and reactions of perimidines and their fused systems. *Curr. Org. Chem.* **2020**, *24*, 1669–1716. [CrossRef]
4. Harry, N.A.; Ujwaldev, S.M.; Aneeja, T.; Anilkumar, G. A comprehensive overview of perimidines: Synthesis, chemical transformations, and applications. *Curr. Org. Chem.* **2021**, *25*, 248–271. [CrossRef]
5. Kalle, P.; Kiseleva, M.A.; Tatarin, S.V.; Smirnov, D.E.; Zakharov, A.Y.; Emets, V.V.; Churakov, A.V.; Bezzubov, S.I. A panchromatic cyclometalated iridium dye based on 2-thienyl-perimidine. *Molecules* **2022**, *27*, 3201. [CrossRef]
6. Ma, Q.; Cai, J.; Mu, S.; Zhang, H.; Liu, K.; Liu, J.; Hong, J. Novel perimidine derivatives as corrosion inhibitors of HRB400 steel in simulated concrete pore solution. *Coatings* **2023**, *13*, 73. [CrossRef]
7. Sahiba, N.; Agarwal, S. Recent advances in the synthesis of perimidines and their applications. *Top. Curr. Chem.* **2020**, *378*, 44. [CrossRef]
8. Yelmame, G.B.; Jagtap, S.B. Review on perimidines: A synthetic pathways approach. *Mater. Sci. Res. India* **2021**, *18*, 14–26. [CrossRef]
9. Mobinikhaledi, A.; Bodaghi Fard, M.A.; Sasani, F.; Amrollahi, M.A. Molecular iodine catalyzed synthesis of some biologically active dihydroperimidines. *Bulg. Chem. Commun.* **2013**, *45*, 353–356.

10. Nagasundaram, N.; Govindhan, C.; Sumitha, S.; Sedhu, N.; Raguvaran, K.; Santhosh, S.; Lalitha, A. Synthesis, characterization and biological evaluation of novel azo fused 2,3-dihydro-1H-perimidine derivatives: In vitro antibacterial, antibiofilm, anti-quorum sensing, DFT, in silico ADME and Molecular docking studies. *J. Mol. Struct.* **2022**, *1248*, 131437. [CrossRef]
11. Arya, K.; Dandia, A. Regioselective synthesis of biologically important scaffold spiro [indole-perimidines]: An antitumor agents. *Lett. Org. Chem.* **2007**, *4*, 378–383. [CrossRef]
12. Wasulko, W.; Noble, A.C.; Popp, F.D. Synthesis of potential antineoplastic agents. XIV. Some 2-substituted 2, 3-dihydro-1h-perimidines. *J. Med. Chem.* **1966**, *9*, 599–601. [CrossRef]
13. Wang, W.-L.; Yang, D.-L.; Gao, L.-X.; Tang, C.-L.; Ma, W.-P.; Ye, H.-H.; Zhang, S.-Q.; Zhao, Y.-N.; Xu, H.-J.; Hu, Z.; et al. 1H–2,3-dihydroperimidine derivatives: A new class of potent protein tyrosine phosphatase 1B inhibitors. *Molecules* **2014**, *19*, 102–121. [CrossRef]
14. Shiraishi, Y.; Yamada, C.; Hirai, T. A coumarin–dihydroperimidine dye as a fluorescent chemosensor for hypochlorite in 99% water. *RSC Adv.* **2019**, *9*, 28636–28641. [CrossRef]
15. Chakraborty, N.; Banik, S.; Chakraborty, A.; Bhattacharya, S.K.; Das, S. Synthesis of a novel pyrene derived perimidine and exploration of its aggregation induced emission, aqueous copper ion sensing, effective antioxidant and BSA interaction properties. *J. Photochem. Photobiol. A Chem.* **2019**, *377*, 236–246. [CrossRef]
16. Fanna, D.J.; Lima, L.M.P.; Craze, A.R.; Trinchi, A.; Wei, G.; Reynolds, J.K.; Li, F. Determination of Cu^{2+} in drinking water using a hydroxyjulolidine-dihydroperimidine colorimetric sensor. *J. Incl. Phenom. Macrocycl. Chem.* **2019**, *94*, 141–154. [CrossRef]
17. Ge, Y.; Zhang, D.; Zhang, X.; Liu, Y.; Du, L.; Wang, Y. A new perimidine-based fluorescent turn-on chemosensor for selective detection of Cu^{2+} ions. *J. Chem. Res.* **2021**, *45*, 125–129. [CrossRef]
18. Hill, A.F.; McQueen, C.M.A. Dihydroperimidine-derived N-heterocyclic pincer carbene complexes via double C–H activation. *Organometallics* **2012**, *31*, 8051–8054. [CrossRef]
19. Hill, A.F.; McQueen, C.M.A. Dihydroperimidine-derived PNP pincer complexes as intermediates en route to N-heterocyclic carbene pincer complexes. *Organometallics* **2014**, *33*, 1909–1912. [CrossRef]
20. McQueen, C.M.A.; Hill, A.F.; Ma, C.; Ward, J.S. Ruthenium and osmium complexes of dihydroperimidine-based N-heterocyclic carbene pincer ligands. *Dalton Trans.* **2015**, *44*, 20376–20385. [CrossRef]
21. Hill, A.F.; Ma, C.; McQueen, C.M.A.; Ward, J.S. Iridium complexes of perimidine-based N-heterocyclic carbene pincer ligands via aminal C-H activation. *Dalton Trans.* **2018**, *47*, 1577–1587. [CrossRef]
22. Malherbe, R.F. 2,3-Dihydroperimidines as Antioxidants for Lubricants. European Patent EP0083311A2, 6 July 1983.
23. Mobinikhaledi, A.; Steel, P.J. Synthesis of perimidines using copper nitrate as an efficient catalyst. *Synth. React. Inorg. Met. Org. Nano Met. Chem.* **2009**, *39*, 133–135. [CrossRef]
24. Varsha, G.; Arun, V.; Robinson, P.P.; Sebastian, M.; Varghese, D.; Leeju, P.; Jayachandran, V.P.; Yusuff, K.K.M. Two new fluorescent heterocyclic perimidines: First syntheses, crystal structure, and spectral characterization. *Tetrahedron Lett.* **2010**, *51*, 2174–2177. [CrossRef]
25. Kalhor, M.; Khodaparast, N. Use of nano-CuY zeolite as an efficient and eco-friendly nano catalyst for facile synthesis of perimidine derivatives. *Res. Chem. Intermed.* **2015**, *41*, 3235–3242. [CrossRef]
26. Bamoniri, A.; Mazoochi, A.; Pourmousavi, S.A. Synthesis of 2,3-dihydroperimidines in the presence of nano-γ-Al_2O_3/BFn and nano-γ-Al_2O_3/BFn/Fe_3O_4 as catalysts under different conditions. *J. Nanostruct.* **2021**, *11*, 554–567. [CrossRef]
27. Khopkar, S.; Shankarling, G. Squaric acid: An impressive organocatalyst for the synthesis of biologically relevant 2,3-dihydro-1H-perimidines in water. *J. Chem. Sci.* **2020**, *132*, 31. [CrossRef]
28. Mannarsamy, M.; Nandeshwar, M.; Muduli, G.; Prabusankar, G. Highly active cyclic zinc(II) thione catalyst for C−C and C−N bond formation reactions. *Chem. Asian J.* **2022**, *17*, e202200594. [CrossRef] [PubMed]
29. Zhang, X.; Liao, S.; Liu, A.; Liu, X.; Kuang, Q.; Wang, Y.; Xu, P.; Huang, X.; Wu, H.; Yuan, J. Imidazolium chloride as an additive for synthesis of perimidines using 1,8-diaminonaphthalene and DMF derivatives. *Tetrahedron Lett.* **2022**, *94*, 153701. [CrossRef]
30. Zhang, B.; Li, J.; Zhu, H.; Xia, X.-F.; Wang, D. Novel recyclable catalysts for selective synthesis of substituted perimidines and aminopyrimidines. *Catal. Lett.* **2022**, *in press*. [CrossRef]
31. Sadri, Z.; Behbahani, F.K.; Keshmirizadeh, E. Synthesis and characterization of a novel and reusable adenine based acidic nanomagnetic catalyst and its application in the preparation of 2-substituted-2,3-dihydro -1*H*-perimidines under ultrasonic irradiation and solvent-free condition. *Polycycl. Aromat. Compd.* **2022**, *in press*. [CrossRef]
32. Kaneti, J.; Kurteva, V.; Georgieva, M.; Krasteva, N.; Miloshev, G.; Tabakova, N.; Petkova, Z.; Bakalova, S.M. Small heterocyclic ligands as anticancer agents: QSAR with a model G-quadruplex. *Molecules* **2022**, *27*, 7577. [CrossRef]
33. Harry, N.A.; Cherian, R.M.; Radhika, S.; Anilkumar, G. A novel catalyst-free, eco-friendly, on water protocol for the synthesis of 2,3-dihydro-1H-perimidines. *Tetrahedron Lett.* **2019**, *60*, 150946. [CrossRef]
34. Bruker, A. *Bruker Advanced X-ray Solutions*; AXS Inc.: Madison, WI, USA, 2016.
35. Bruker, A. *Saint and SADABS*; Bruker AXS Inc.: Madison, WI, USA, 2009.
36. Sheldrick, G.M. SHELXT–Integrated space-group and crystal-structure determination. *Acta Cryst. Sect. A* **2015**, *71*, 3–8. [CrossRef]
37. Sheldrick, G.M. Crystal structure refinement with SHELXL. *Acta Cryst. Sect. C* **2015**, *71*, 3–8. [CrossRef]
38. Dolomanov, O.V.; Bourhis, L.J.; Gildea, R.J.; Howard, J.A.; Puschmann, H. OLEX2: A complete structure solution, refinement and analysis program. *J. Appl. Crystallogr.* **2009**, *42*, 339–341. [CrossRef]
39. Farrugia, L.J. WinGX and ORTEP for Windows: An update. *J. Appl. Crystallogr.* **2012**, *45*, 849–854. [CrossRef]

40. Macrae, C.F.; Sovago, I.; Cottrell, S.J.; Galek, P.T.; McCabe, P.; Pidcock, E.; Platings, M.; Shields, G.P.; Stevens, J.S.; Towler, M. Mercury 4.0: From visualization to analysis, design and prediction. *J. Appl. Crystallogr.* **2020**, *53*, 226–235. [CrossRef]
41. Spackman, P.R.; Turner, M.J.; McKinnon, J.J.; Wolff, S.K.; Grimwood, D.J.; Jayatilaka, D.; Spackman, M. CrystalExplorer: A program for Hirshfeld surface analysis, visualization and qu antitative analysis of molecular crystals. *J. Appl. Crystallogr.* **2021**, *54*, 1006–1011. [CrossRef]
42. Mackenzie, C.F.; Spackman, P.R.; Jayatilaka, D.; Spackman, M.A. CrystalExplorer model energies and energy frameworks: Extension to metal coordination compounds, organic salts, solvates and open-shell systems. *IUCrJ* **2017**, *4*, 575–587. [CrossRef]
43. Jayatilaka, D.; Grimwood, D.J. Tonto: A Fortran Based Object-Oriented System for Quantum Chemistry and Crystallography. In *International Conference on Computational Science*; Springer: Berlin/Heidelberg, Germany, 2003; pp. 142–151. [CrossRef]